ELSEVIER

Polymer 40 (1999) 3657–3663

polymer

Strain recovery mechanism of PBT/rubber thermoplastic elastomer

Takashi Aoyama[a], Angola Juan Carlos[a], Hiromu Saito[a], Takashi Inoue[a,*], Yasushi Niitsu[b]

[a]*Department of Organic and Polymeric Materials, Tokyo Institute of Technology, Ookayama, Meguro-ku, Tokyo 152-8552, Japan*
[b]*Department of Mechanical Engineering, Tokyo Denki University, Kanda-nishiki-cho, Chiyoda-ku, Tokyo 101-8457, Japan*

Received 20 February 1998; received in revised form 1 June 1998; accepted 11 August 1998

Abstract

The thermoplastic elastomer (TPE) prepared by dynamic vulcanization is a two-phase material in which crosslinked rubber particles are densely dispersed in a ductile polymer matrix. The TPE shows an excellent strain recovery, even though the matrix consists of ductile plastics. This behavior was exemplified in a 50/50 poly(butylene terephthalate)(PBT)/ethylene rubber blend. Finite element method (FEM) analysis revealed that: (1) the low stress evolved in PBT matrix with bulk deformation, especially in the ligament matrix between rubber particles in stretching direction, is locally preserved within an elastic limit and it acts as an in situ formed adhesive for interconnecting the rubber particles, and (2) the volumeric strain of rubber particles with high Poisson's ratio provides the contractile stress to heal the plastically deformed PBT phase outside the ligament matrix. Such strain mechanisms were supported by the polarized FT-Raman spectroscopy in terms of the peak shift caused by chain distortion, its anisotropy, and the gauche-to-trans transformation associated with plastic deformationm, in comparison with those in neat PBT.

Keywords: Thermoplastic elastomer; Poly(butylene terephthalate); Stress distribution

1. Introduction

Thermoplastic elastomer (TPE) prepared by dynamic vulcanization is a two-phase material in which cured rubber particles are densely dispersed in a matrix of ductile polymer. It can be melt-processed at high temperature and behaves like a vulcanized rubber at ambient temperature [1,2]. The question is on its excellent strain recovery, i.e., why the TPE can shrink back from the highly deformed state, even though the matrix consists of a ductile polymer. In other words, why is the bulk property of the TPE not governed by the ductile character of the matrix but mostly by that of the dispersed phase?

In order to answer this question, a two-dimensional (2d) elastic–plastic analysis by two-dimensional finite element method (FEM) has been carried out on the deformation mechanism of TPE. The 2d-FEM analysis revealed that, even in the highly deformed states, the ligament matrix between rubber particles in the stretching direction is locally preserved within an elastic limit and it acts as an in situ formed adhesive for interconnecting rubber particles [3,4].

In this paper, we extend the FEM analysis to a three-dimensional (3d) version to get better understanding of the local stresses evolved in the two-phase material. Then, the FEM results are tested by an optical method; i.e., the stresses and the distribution evolved with the bulk deformation are estimated by the polarized Fourier transform (FT) Raman spectroscopy. When the stress is applied for polymer chain, the chain distortion causes a frequency shift in Raman spectrum [5–14]. Using the polarized FT-Raman spectroscopy, one can estimate the anisotropy of stress evolved in polymers. TPE employed in this study is a blend of poly(butylene terephthalate) (PBT) with poly(ethylene-co-glycidyl methacrylate) rubber prepared by dynamic vulcanization [4].

2. Experimental

2.1. Materials

The PBT used in this study was a commercial polymer supplied by Toyobo Co., Ltd ($Mn = 4.7 \times 10^4$). The rubber was a poly(ethylene-co-glycidyl methacrylate) copolymer supplied by Sumitomo Chemical Co., Ltd (Bondfast; methacrylate content = 3 mol%). The curing agent for the rubber was adipic acid, which reacts with the epoxy group.

2.2. Blend preparation

In order to obtain the dynamically vulcanized blend, PBT

* Corresponding author.

0032-3861/99/$ - see front matter
PII: S0032-3861(98)00585-0

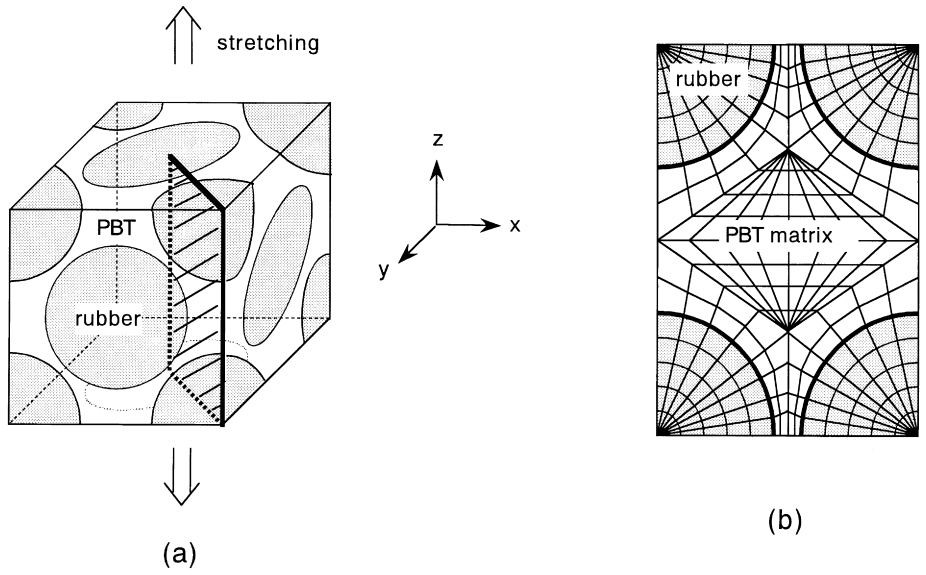

Fig. 1. Three-dimensional FEM model for 50/50 PBT/rubber blend: (a) FCC cube with 14 rubber inclusions, (b) two-dimensional plane with FEM mesh sliced from (a).

and rubber were melt-mixed in the presence of adipic acid (content of adipic acid was 0.4 phr) at 260°C for 15 min by using a Mini-Max molder (CSI-183 MMX, Custom Scientific Instruments, Inc.). The blend ratio of PBT and rubber was fixed at 50/50 weight ratio. Neat PBT and the PBT/rubber blends were compression-molded at 260°C into thick film about 1 mm thickness, and then they were rapidly quenched in an ice water bath. The film was cut into a rectangle of length 50 mm and width 3 mm.

2.3. Mechanical test

The stress–strain curve of the film specimen was measured by using a tensile testing machine (Tensilon UTM-II-20, Toyo Boldwin Co. Ltd) at a constant strain rate of 200% min^{-1} at room temperature, both for stretching and releasing processes. After the specimen was stretched to a fixed strain (50%), the stretched specimen was held at this strain for 1 min and then released to shrink back.

2.4. Transmission electron microscopy

For transmission electron microscopic observation, ultrathin sections of 70 nm thickness were cut from the film specimens and stained with ruthenium tetraoxide ($Ru0_4$) in the gas phase at room temperature for 20 h. The phase structure in the section was observed under a JEM-100CX electron microscope (JEOL Ltd) with an accelerator voltage of 100 kV.

2.5. Polarized FT-Raman measurement

Polarized FT-Raman measurement was carried out with an RFT-800 spectrometer (Japan Spectroscopic Co. Ltd) equipped with a compact stretching device. Spectra were obtained at a resolution of 2 cm^{-1} using the 1064 nm line of a 1 W Nd:YAG laser in a 180° backscattering geometry [14,15]. The backscattering light was detected by a thermoelectrically cooled InGaAs detector. The stretching device was rotated to provide two polarization modes: one was the Vv in which polarizer and analyzer were parallel to the stretching direction and the other was the Hh in which polarizer and analyzer were perpendicular to the stretching direction [8]. Both crossheads of the stretching device travelled at the same speed so that the laser irradiated a fixed point of the specimen throughout the stretching and releasing process.

2.6. FEM analysis

The elastic-plastic analysis for the deformation mechanism of PBT/rubber TPE was carried out by 3d-FEM using a non-linear computer program, NISA II.

A 3d-model constructed for FEM analysis is shown in Fig. 1. Fourteen particles of rubber were embedded in a PBT matrix in a face-centered cubic (FCC) arrangement (Fig. 1(a)). The volume ratio of PBT/rubber was set at 42/58 which was calculated for 50/50 PBT/rubber ratio by taking into account the density of each component polymer (density of PBT is 1.31 g/ml and that of rubber is 0.964 g/ml). Each element was assumed to have the mechanical property identical to that of the neat component polymer. That is, it was assumed that the element exhibits the same true stress (σ)–true strain (ε') curve observed for the component polymer. To simplify the FEM numerical calculation, the $\sigma-\varepsilon'$ curve was approximated to be composed of two straight lines, as described in the previous paper [4]. The Poisson's ratio of PBT was assumed to be 0.37 and that of rubber was 0.49. Adhesive strength at the interface

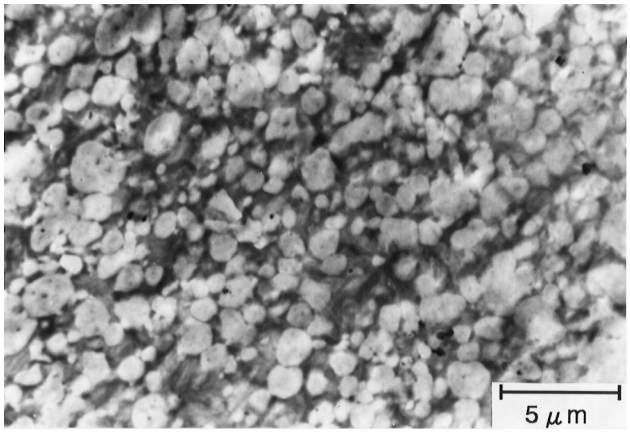

Fig. 2. Transmission electron micrograph of a 50/50 PBT/rubber blend by dynamic vulcanization.

between PBT and rubber phases was assumed to be infinitely strong.

The FEM model was uniaxially stretched in the *z*-direction. Stresses evolved at *x*, *y*, and *z* directions; σ_x, σ_y, and σ_z, and a shear stress τ_{xy}, τ_{yz}, τ_{zx} were calculated for each element as a function of bulk strain. In order to display the stress for the 3d-FEM model, the stress on a plane sliced from the cube (Fig. 1(a)) was obtained (Fig. 1(b)). Also calculated was the equivalent stress $\bar{\sigma}$ defined by

$$\bar{\sigma} = \{\tfrac{1}{2}[(\sigma_x - \sigma_y)^2 + (\sigma_y - \sigma_z)^2 + (\sigma_z - \sigma_x)^2 + 6(\tau_{xy}^2 + \tau_{yz}^2 + \tau_{zx}^2)]\}^{\frac{1}{2}} \quad (1)$$

where $\bar{\sigma}$ is assumed to be a reduced tensile stress which is equivalent to the triaxial stress.

3. Results and discussion

Fig. 2 shows the transmission electron micrograph of the 50/50 PBT/rubber blend prepared by the dynamic vulcanization. Since RuO_4 stains just PBT, the dark matrix is assigned to PBT phase, while bright particles to rubber particles. One sees clearly the dispersion of rubber particles in the PBT matrix. The fine dispersion of rubber may be caused by the reaction between the epoxy group of rubber and the carboxylic acid end-group of PBT in the dynamic vulcanization process to yield an in situ formed PBT–rubber graft copolymer, which will suppress the coagulation of rubber particles [4].

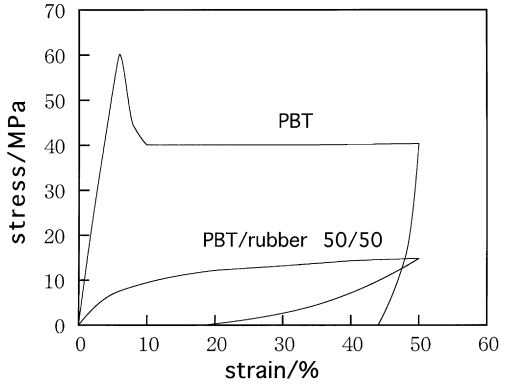

Fig. 3. Stress–strain behavior for the stretching and releasing processes of neat PBT and 50/50 PBT/rubber blend.

Fig. 3 shows the stress–strain curve for the stretching and releasing processes in neat PBT and 50/50 PBT/rubber. When neat PBT is stretched above the yield point at $\varepsilon = 10\%$, plastic deformation takes place, and then it hardly recovers after releasing at $\varepsilon = 50\%$. On the other hand, the blend exhibits excellent strain recovery; i.e., the blend can shrink back from the highly deformed state even though the matrix consists of a ductile polymer PBT.

In Fig. 4 is shown a typical example of the contour plots of the stress parallel to the stretching direction σ_z and that perpendicular to the stretching one σ_x. The stress in the stretching direction is positive (Fig. 4(a)), indicating that the elongational stress is applied in the stretching direction. On the other hand, the stress is negative in the perpendicular direction (Fig. 4(b)), indicating that the compressive stress is applied in the perpendicular direction.

The stress distributions obtained by Fig. 4 are shown in Fig. 5. Such distributions are displayed to compare the FEM results with those by FT-Raman analysis. The stress distributions are wide in both directions. Elongational stress is dominated in the stretching direction while compressive stress is dominant in the perpendicular direction. The average stress in the stretching direction is only 56 MPa, while that in the neat PBT is 110 MPa, indicating that the applied stress on the PBT matrix in the blend is much smaller than that of the neat PBT.

The equivalent stress $\bar{\sigma}$ calculated by Eq. (1) is shown in Fig. 6. Here the von Mises criterion for yielding was applied for the FEM elements; i.e., the matrix elements' yield when the equivalent stress $\bar{\sigma}$ exceeds the yield stress σ_Y of neat PBT ($\sigma_Y = 62$ MPa). The elements at which $\bar{\sigma}$ is larger than σ_Y are shaded in Fig. 6. The yielding is induced at the equatorial region of the PBT matrix between rubber particles. It is interesting that, even at $\varepsilon = 50\%$, the meridional region of the PBT matrix still remains unyielded. That is, the PBT matrix is locally preserved at low stress ($\bar{\sigma} < \sigma_Y$) within the elastic limit. It will partly help the elastic recovery. However, it seems to be insufficient to heal the yielded region of PBT matrix. The healing may be caused by another mechanism, as shown in the next figure.

Fig. 7 shows the stress in the stretching direction σ_z at releasing process: at $\varepsilon = 32.5\%$ after stretching to $\varepsilon = 50\%$ and releasing. One sees a big change in stress distribution from Fig. 4(a). The stress in the center of the matrix is negative; i.e., contractile force is generated for the healing. Actually, the length of the FEM model in Fig. 7 in the stretching direction is shortened, compared with that in Fig. 6. The elastic recovery really takes place, as we discussed in a previous paper [4]. The contractile stress

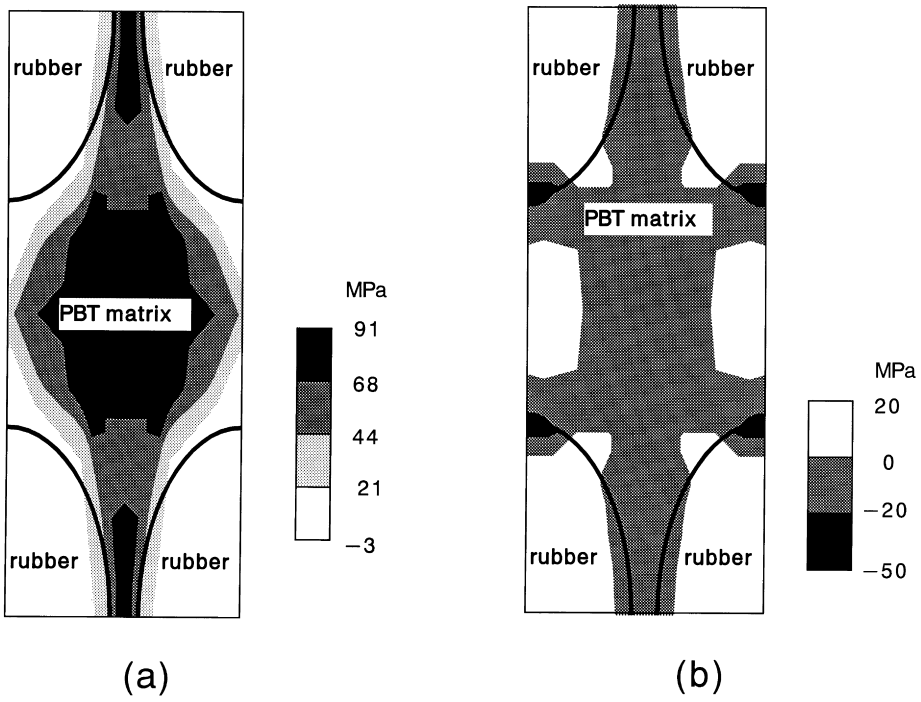

Fig. 4. Contour plot of the stress at $\varepsilon = 50\%$: (a) parallel to the stretching direction, (b) perpendicular to the stretching direction.

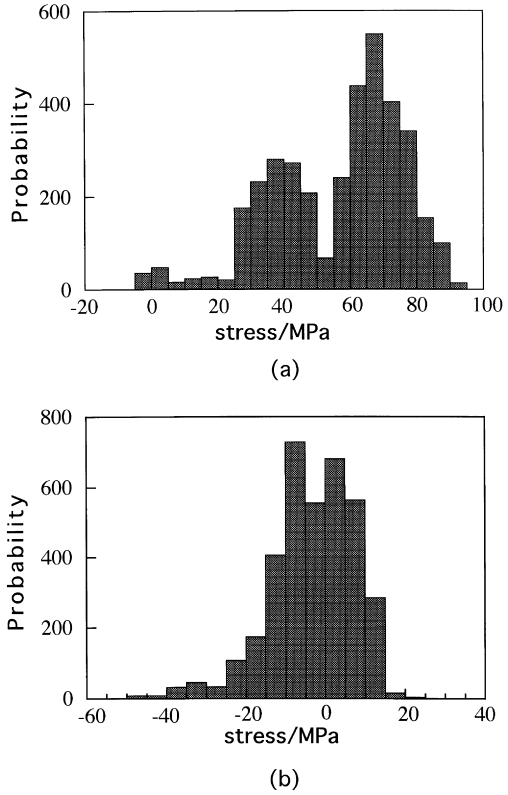

Fig. 5. Stress distribution at $\varepsilon = 50\%$; (a) parallel to the stretching direction, (b) perpendicular to the stretching direction.

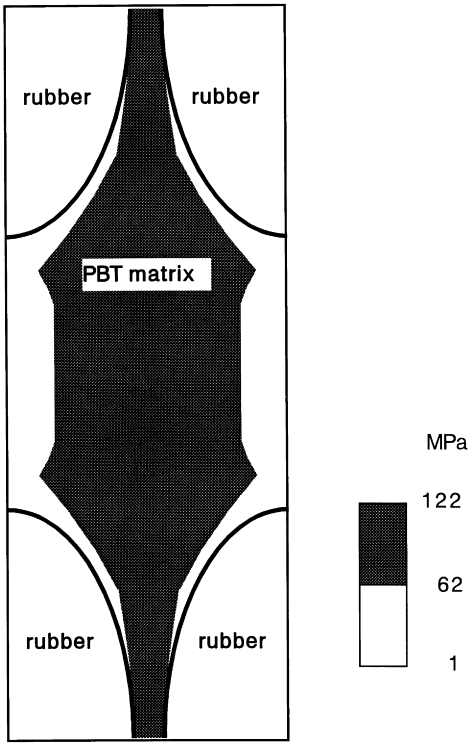

Fig. 6. Contour plot of the equivalent stress $\bar{\sigma}$ by Eq. (1) at $\varepsilon = 50\%$. Yield elements are shaded.

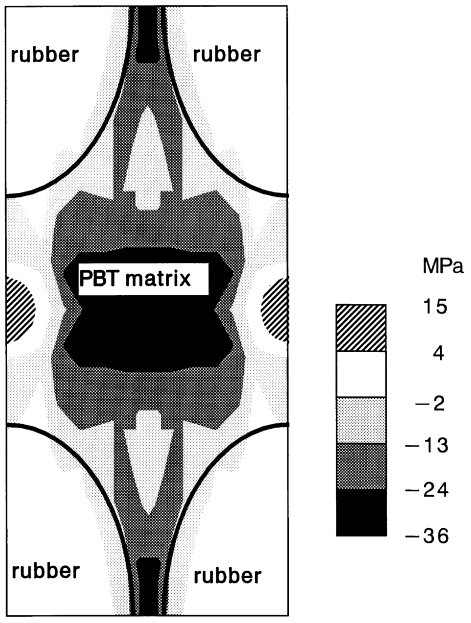

Fig. 7. Contour plot of the stress in the stretching direction at $\varepsilon = 32.5\%$ after stretching to $\varepsilon = 50\%$ and releasing.

could be provided by the volumeric strain of the rubber particles which have a high Poisson's ratio (≈ 0.5; very small volume change with deformation).

Anyhow, the FEM analysis suggests that the stress concentration in the PBT matrix results in the yielding, but the yielded PBT matrix can be healed to render the elastic recovery of the two-phase material. Such a strain recovery mechanism could be justified by analyzing the stress distribution by FT-Raman spectroscopy and comparing the results with those by FEM analysis, as follows.

In order to characterize the applied stress on PBT chains, we chose the C–C stretching band of a phenylene ring [16] at 1615 cm^{-1} as a stress sensitive Raman band. Fig. 8 shows a typical example of the spectra in a wavenumber range of C–C stretching band of a phenylene ring for unstretched and

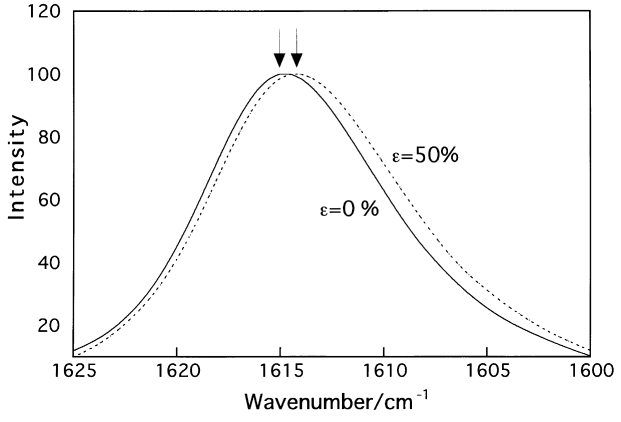

Fig. 8. FT-Raman spectra covering the wavenumber range of the C–C stretching band of phenylene ring in neat PBT; unstretched and stretched state.

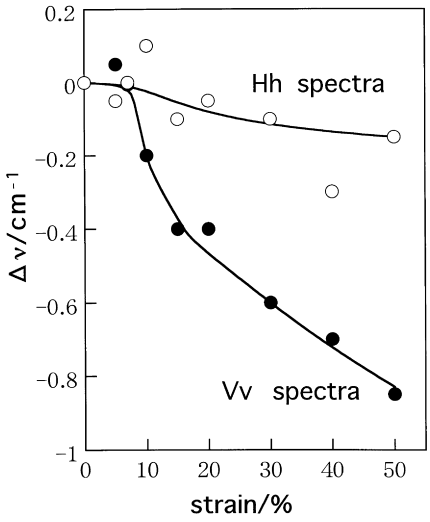

Fig. 9. Peak shift $\Delta\nu$ of the C–C stretching band of phenylene ring as a function of strain for stretching process in neat PBT.

stretched state of neat PBT. The peak position shifts to a smaller wavenumber by stretching. The peak shift is caused by the applied stress associating with the chain distortion. The magnitude of the shift increases with increasing stress [5–14].

The peak shift $\Delta\nu$ was evaluated by the wavenumber difference of the peak position for the stretched state from that for the unstretched state. Fig. 9 shows the peak shift $\Delta\nu$ of the neat PBT thus obtained as a function of strain ε for Vv and Hh spectra. The strain dependence of the $\Delta\nu$ for the Vv spectra can be divided into three stages. The peak position hardly changes with ε at small ε up to $\varepsilon = 10\%$. At around $\varepsilon = 15\%$, the peak position shifts steeply, and then it shifts gradually at higher strain ($\varepsilon > 20\%$). According to Rodríquez-Cabello et al. [14], the first stage corresponds to the elastic region, the second stage to the transient region from elastic to plastic deformation, and the third stage to the plastic deformation region. The steep shift at the second stage may be ascribed to the change of the conformation from gauche to trans (see Fig. 12) associated with the chain distortion. On the other hand, the shift is a little for the Hh spectra. The Vv spectra is contributed to from the chains parallel to the stretching direction while the Hh one is from the chains perpendicular to the stretching direction [8]. Thus, the results suggest that the applied stress is large in the stretching direction, while it is small in the perpendicular direction.

The ε dependence of the peak shift $\Delta\nu$ of the PBT matrix in the blend is shown in Fig. 10. The peak position shifts monotonously with strain at small strain up to $\varepsilon = 20\%$, and then it levels off. The interesting result here is that the peak shift for the Vv spectra is opposite to that for the Hh one; i.e., the peak shifts to higher wavenumber in the Hh spectra while it shifts to lower wavenumber in the Vv spectra. The result suggests that the compressive stress is evolved in the direction perpendicular to the stretching direction, while

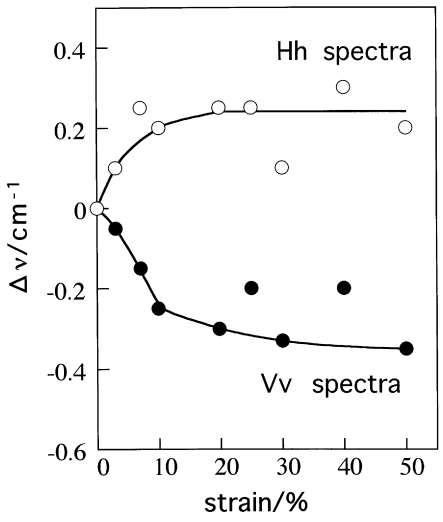

Fig. 10. Peak shift $\Delta\nu$ of the C–C stretching band of phenylene ring as a function of strain for stretching process in 50/50 PBT/rubber blend.

elongational stress in the stretching direction. This is exactly the situation simulated by FEM analysis (4). Also note that the magnitude of $\Delta\nu$ in the blend is much smaller than that in the neat PBT. It suggests that the stress level in the blend is smaller than that in the neat PBT. This is again what we simulated by FEM analysis.

Fig. 11 shows the spectra of a neat PBT in a wavenumber range of 820–900 cm^{-1} for the unstretched state and stretched state at $\varepsilon = 50\%$. The peak at 886 cm^{-1} is the C–H rocking band [16] and it disappears at high strain. The change of the peak intensity is ascribed to the change from gauche conformation to trans, associating with the plastic deformation [17]. To estimate the degree of gauche-to-trans transformation, we calculated the ratio R of the peak intensity I at 886 cm^{-1} to that at 860 cm^{-1}; $R = I(886\ cm^{-1})/I(860\ cm^{-1})$.

Fig. 12 shows the decrease in normalized R with deformation, $[R(\varepsilon) - R(\varepsilon = 0)]/R(\varepsilon = 0)$. In neat PBT, the trans conformation increases steeply above $\epsilon = 10\%$ with strain and almost all of the gauche conformers change to trans

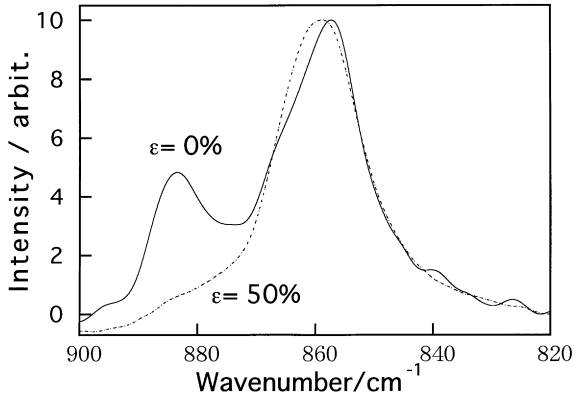

Fig. 11. FT-Raman spectra covering the wavenumber range of the C–H rocking band in neat PBT; unstretched and stretched states.

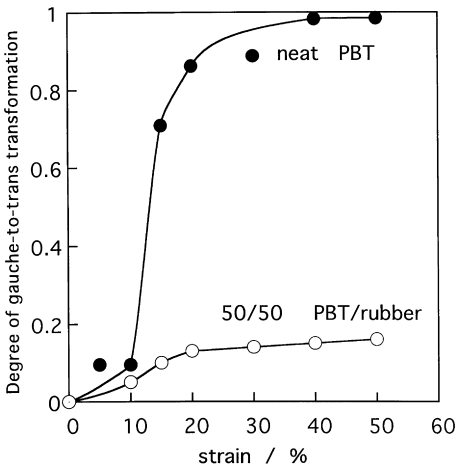

Fig. 12. Gauche-to-trans transformation associated with bulk deformation in neat PBT and 50/50 PBT/rubber blend.

above $\varepsilon = 20\%$. On the other hand, the increase of the trans conformation is a little in the blend even at $\varepsilon = 50\%$, suggesting again that the stress level in the blend is much lower than that in neat PBT (5). Some parts in the PBT matrix in the blend are preserved within an elastic limit (Fig. 6). The results are in good agreement with the FEM results.

Fig. 13 shows the change in Vv spectra of the blend with stretching and releasing. The spectra are shifted vertically for clarity. The peak position shifts to lower wavenumber by stretching ($\varepsilon = 50\%$), and then it shifts to higher wavenumber by releasing ($\varepsilon = 40\%$). Note that the peak position for the released state is higher than that of the unstretched state. The results suggest the evolution of contractile stress during the releasing process, as expected from the FEM analysis (Fig. 7).

4. Conclusion

On the basis of FEM analysis, the key mechanisms of strain recovery in TPE are: (1) the low stress evolved in the PBT matrix with bulk deformation, especially in the ligament matrix between rubber particles in the stretching

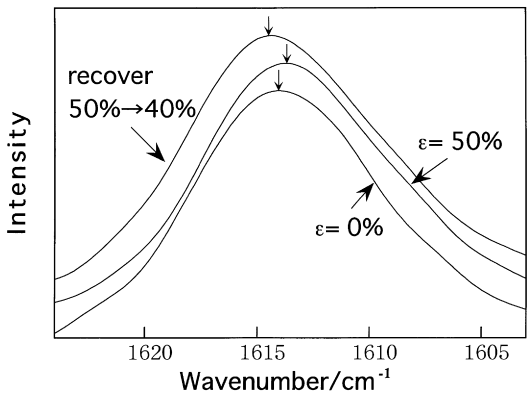

Fig. 13. Change in FT-Raman spectrum of 50/50 PBT/rubber blend with stretching and releasing.

direction, is locally preserved within an elastic limit and it acts as an in situ formed adhesive for interconnecting the rubber particles, and (2) the volumeric strain of rubber particles with high Poisson's ratio provides the contractile stress to heal the plastically deformed PBT phase outside the ligament matrix. Such mechanisms were spectroscopically supported by the polarized FT-Raman studies.

References

[1] Coran AY. In: Bhomwick AK, Stephens HL. Handbook of elastomers—new developments and technology. New York: Marcel Dekker, 1988.
[2] Holden G, Legge NR, Quirk RP, Schroeder HE, editors. Thermoplastic elastomers, 2nd ed. Munich: Hanser, 1996.
[3] Kikuchi Y, Fukui T, Okada T, Inoue T. Polym Eng Sci 1991;31:1029.
[4] Okamoto M, Shiomi K, Inoue T. Polymer 1994;35:4618.
[5] Wool RP, Boyd RH. J Appl Phys 1980;51:5116.
[6] Wool RP, Bretzlaff RS, Li BY, Wang CH, Boyd RH. J Polym Sci, Polym Phys Edn 1986;24:1039.
[7] Day RJ, Robinson IM, Zakikhani M, Young RJ. Polymer 1987;28:1833.
[8] Fina LJ, Bower DI, Ward IM. Polymer 1988;29:2146.
[9] Tashiro K, Wu G, Kobayashi M. J Polym Sci Polym Phys Edn 1990;28:2527.
[10] Young RJ, Day RJ, Dong L, Knoff W. J Mater Sci 1992;27:5431.
[11] Hu X, Stanford JL, Day RJ, Young RJ. Macromolecules 1992;25:684.
[12] Tashiro K, Minami S, Wu G, Kobayashi M. J Polym Sci, Polym Phys Ed 1992;30:1143.
[13] Tashiro K, Kobayashi M, Tadokoro H. Polym Eng Sci 1994;34:308.
[14] Rodríquez-Cabello JC, Merino JC, Jawhari T, Pastor JM. Polymer 1995;36:4233.
[15] Pigeon M, Prud'homme RE, Pézolet M. Macromolecules 1991;24:5687.
[16] Ward IM, Wilding MA. Polymer 1977;18:327.
[17] Hutchinson IJ, Ward IM, Willis HA, Zichy V. Polymer 1980;21:55.